

Accepted Manuscript

Removal of pharmaceutical compounds, artificial sweeteners, and perfluoroalkyl substances from water using a passive treatment system containing zero-valent iron and biochar

YingYing Liu, David W. Blowes, Carol J. Ptacek, Laura G. Groza



PII: S0048-9697(19)33023-2
DOI: <https://doi.org/10.1016/j.scitotenv.2019.06.450>
Reference: STOTEN 33104
To appear in: *Science of the Total Environment*
Received date: 10 April 2019
Revised date: 15 June 2019
Accepted date: 26 June 2019

Please cite this article as: Y. Liu, D.W. Blowes, C.J. Ptacek, et al., Removal of pharmaceutical compounds, artificial sweeteners, and perfluoroalkyl substances from water using a passive treatment system containing zero-valent iron and biochar, *Science of the Total Environment*, <https://doi.org/10.1016/j.scitotenv.2019.06.450>

This is a PDF file of an unedited manuscript that has been accepted for publication. As a service to our customers we are providing this early version of the manuscript. The manuscript will undergo copyediting, typesetting, and review of the resulting proof before it is published in its final form. Please note that during the production process errors may be discovered which could affect the content, and all legal disclaimers that apply to the journal pertain.

Removal of Pharmaceutical Compounds, Artificial Sweeteners, and Perfluoroalkyl Substances from Water Using a Passive Treatment System Containing Zero-valent Iron and Biochar

YingYing Liu, David W. Blowes, Carol J. Ptacek*, and Laura G. Groza

Department of Earth and Environmental Sciences, University of Waterloo, Waterloo, Ontario, Canada N2L 3G1

* Corresponding author. Tel.: +1 519 888 4567x32230; fax: +1 519 746 7484

E-mail address: ptacek@uwaterloo.ca

Present address: Department of Earth and Environmental Sciences, 200 University Avenue West, Waterloo, Ontario, Canada N2L 3G1

Abstract:

Emerging contaminants are widely detected and persistent in environmental waters. Advanced oxidation processes are among the most effective methods for removing emerging contaminants from water; however, high energy consumption greatly increases the operating costs and limits large-scale applications. In this study, a passive treatment system consisting of four columns packed with mixtures of silica sand, zero-valent iron (ZVI), biochar (BC), and a mixture of (ZVI + BC) were evaluated for simultaneous removal of eight pharmaceuticals, four artificial sweeteners, and two perfluoroalkyl substances (PFASs) from water. Overall, the passive treatment system was more effective for removing target pharmaceuticals (almost complete removal) than artificial sweeteners and PFASs (partial removal). Columns *ZVI*, *BC*, and (*ZVI* + *BC*) exhibited similar effective removal (>97%) of target pharmaceuticals, including carbamazepine, caffeine, sulfamethoxazole, 3,4-methylenedioxyamphetamine, 3,4-methylenedioxymethamphetamine, ibuprofen, gemfibrozil, and naproxen, from ~9 to < 0.25 $\mu\text{g L}^{-1}$; pharmaceuticals were more rapidly removed by Columns *ZVI* and (*ZVI* + *BC*) than Column *BC*, except for ibuprofen. Column *ZVI* was more effective for removing artificial sweeteners acesulfame-K and sucralose than Columns *BC* and (*ZVI* + *BC*); however, *BC* exhibited relatively greater removal of saccharin than *ZVI* and (*ZVI* + *BC*). Acesulfame-K and saccharin (~110 $\mu\text{g L}^{-1}$) were partially removed in the treatment columns. Cyclamate was not removed in any of the columns. However, more than 76% of input sucralose (~110 $\mu\text{g L}^{-1}$) was removed in the three treatment columns. Reactive medium *BC* alone was more effective for removing target PFASs than *ZVI* and (*ZVI* + *BC*). Input perfluorooctanoic acid (PFOA) (~45 $\mu\text{g L}^{-1}$) was partially removed in the columns containing *BC* but not *ZVI* alone. Between 10 and 80% of input

perfluorooctane sulfonic acid (PFOS) ($24\text{--}90\ \mu\text{g L}^{-1}$) was removed in Column *ZVI*; greater removals ($57\text{--}99\%$) were observed in Columns *BC* and (*ZVI + BC*).

Keywords: pharmaceutical compounds; artificial sweeteners; perfluoroalkyl substances; zero-valent iron; biochar; passive treatment system

1. Introduction

Pharmaceuticals and artificial sweeteners are heavily consumed by society. These compounds pass through human digestive tracts and end up in treated wastewater as unchanged parent compounds or degradation products. However, at many locations, conventional wastewater treatment systems cannot efficiently remove these emerging contaminants from water (Metcalf et al., 2003; Scheurer et al., 2009). This has resulted in the ubiquitous occurrence of pharmaceuticals (such as carbamazepine (CBZ), caffeine (CAF), sulfamethoxazole (SMX), ibuprofen (IBU), gemfibrozil (GEM), and naproxen (NAP)) and artificial sweeteners (such as acesulfame-K (ACE-K), cyclamate (CYC), sucralose (SCL), and saccharin (SAC)) in the environment (Rodil et al., 2012; Zhao et al., 2017). The concentrations of pharmaceuticals and artificial sweeteners in environmental waters such as surface water and groundwater are usually in the range of ng L^{-1} to $\mu\text{g L}^{-1}$, with relatively higher concentrations observed in wastewater derived from domestic and municipal sources. Metcalfe et al. (2003) report that up to $2\ \mu\text{g L}^{-1}$ of CBZ, $5\ \mu\text{g L}^{-1}$ of GEM, and $40\ \mu\text{g L}^{-1}$ of NAP and IBU are detected in the influents and effluents of 14 Canadian sewage treatment plants. Carrara et al. (2008) observe up to $7\ \mu\text{g L}^{-1}$ of IBU, GEM, and NAP in the septic system of Long Point Provincial Park, Ontario, Canada; later, Van Stempvoort et al. (2011) report up to $100\ \mu\text{g L}^{-1}$ of artificial sweeteners ACE-K, CYC, SCL, and SAC observed in the contaminated groundwater at the same site. Due to the persistence of some pharmaceuticals and artificial sweeteners, they have been used to track anthropogenic

contamination in aquatic environments (James et al., 2016; Liu et al., 2014a; Van Stempvoort et al., 2013).

Perfluoroalkyl substances (PFASs) are primarily used as surfactants in industrial, military, and consumer products such as polymer additives, surface treatment agents, and fire retardants because of their high thermal and chemical stability (Ahrens, 2011). These compounds are extremely persistent and resistant to physical, chemical, and biological degradation and have been reported to be transported globally (Rahman et al., 2014). Perfluorooctanoic acid (PFOA; $C_7F_{15}COOH$) and perfluorooctane sulfonic acid (PFOS; $C_8F_{17}SO_3^-$) are the most studied PFASs because of their frequent detection and high observed concentrations. These contaminants have been widely found in wastewater, surface water, groundwater, and drinking water in the range of $ng\ L^{-1}$ to $\mu g\ L^{-1}$ (Ahrens, 2011; Schaider et al., 2014). Relatively higher concentrations of PFOA and PFOS are usually detected near industrial or municipal wastewater treatment plants (WWTPs), landfill leachate, airports, military bases, and manufacturing facilities. As an example, Anderson et al. (2016) report up to $250\ \mu g\ L^{-1}$ of PFOA and $8970\ \mu g\ L^{-1}$ of PFOS in the surface water and groundwater close to U.S. Air Force bases that utilized aqueous film-forming foams.

Pharmaceutical compounds and PFASs have been reported to be reproductive and developmental toxicants and endocrine disruptors; moreover, PFASs are bioaccumulative and possibly carcinogenic (Ding and Peijnenburg, 2013; Sanchez et al., 2011). Because most drinking water and wastewater treatment systems (except for reverse osmosis and nanofiltration) cannot efficiently remove pharmaceuticals (e.g., CBZ, CAF, and IBU), artificial sweeteners (e.g., ACE-K and SCL), and especially PFASs (e.g., PFOA and PFOS), different technologies such as advanced oxidation, microbial treatment, and granular activated carbon (GAC) adsorption have been extensively studied for removing these contaminants from water (Ahmed et al., 2016; Bo et

al., 2015; Merino et al., 2016). Advanced oxidation processes (AOPs) such as UV photo- and photocatalytic degradation and UV/H₂O₂, ozonation can effectively degrade many pharmaceuticals and artificial sweeteners (Sharma et al., 2014; Tong et al., 2012). The degradation or decomposition of PFASs is more challenging than for other emerging contaminants due to the highly stable saturated C-F bond. Treatment methods for removing PFASs, such as AOPs (Hori et al., 2006) or nanofiltration and GAC (Appleman et al., 2013), either require strong oxidizing radicals ($\cdot\text{OH}$ and $\text{SO}_4^{\cdot-}$) under extreme conditions such as low pH, high temperature, and high pressure or need to be frequently changed or renewed, which makes these methods costly and less effective in field applications.

ZVI is a strong reductant (reduction potential of -0.44 V) and has the potential to degrade environmental contaminants, such as nitro-organic compounds and chlorinated hydrocarbons (Jeen et al., 2013; Liu et al., 2018). Limited studies have reported the use of ZVI alone as a reducing agent for removing pharmaceuticals and PFASs from water. König et al. (2016) demonstrate reductive biotransformation of the pharmaceutical CBZ using ZVI sponge material with 20% removal. Reductive degradation (38–96% removed) of four PFASs (PFOA, PFNA, PFDA, and PFOS) has been reported using Mg-amino clay coated nanoscale ZVI under low pH (pH 3) conditions (Arvaniti et al., 2015).

Biochar (BC) is a porous carbon residue derived from waste organic materials. BC has a large surface area and high porosity, and contains various functional groups (carboxylic, aliphatic, and phenolic groups) that provide exchange sites for the adsorption of cations, heavy metals, and anions. In addition, the high carbon content makes biochar an effective sorbent for nonpolar organic compounds in wastewater treatment (Scherer et al., 2000). Several studies report effective sorption of pharmaceuticals CBZ, SMX, IBU, and NAP and perfluorinated

compounds by BC (Jung et al., 2015; Kupryianchyk et al., 2016; Rajapaksha et al., 2015; Williams et al., 2015).

ZVI and BC are non-toxic and cost-effective reactive materials and easy to obtain. The purpose of this study was to evaluate the potential of these reactive materials for the simultaneous removal of three classes of emerging contaminants under dynamic flow conditions. Four column experiments were conducted to evaluate the removal of pharmaceuticals ($\sim 10 \mu\text{g L}^{-1}$), artificial sweeteners ($\sim 100 \mu\text{g L}^{-1}$), and perfluoroalkyl substances ($20\text{--}100 \mu\text{g L}^{-1}$) from simulated groundwater using ZVI, BC, and a mixture thereof. The target contaminants and their concentrations were selected and chosen according to their occurrences and concentrations found in wastewaters derived from domestic and municipal sources (Ahrens, 2011; Carrara et al., 2008; Metcalfe et al., 2003; Van Stempvoort et al., 2011).

2. Materials and Methods

2.1 Column Design and Experimental Setup

The four acrylic columns each had a length of 30 cm and internal diameter of 5 cm. Ports were attached to the bottom and top of each column to respectively introduce influent and discharge effluent solutions. Seven sampling ports were installed along the length of each column at 3.75-cm intervals. Column *Control* was packed with 100% silica sand (SS). Column *ZVI* was packed with 50% (v/v) granular ZVI and 50% (v/v) SS. Column *BC* was packed with 50% (v/v) BC and 50% (v/v) SS. Column (*ZVI + BC*) was packed with 10% (v/v) granular ZVI, 40% (v/v) BC, and 50% (v/v) SS. The SS was used as supporting material. The proportion of SS, ZVI, and BC in four columns was adopted from previously published studies (Benner et al., 1999; Benner et al., 1997; Gillham and O'Hannesin, 1994; Liu et al., 2014b). A 1 cm-thick layer of 100% SS was packed on the top and bottom ends of the columns to separate the column packing from the

influent and effluent ports. The physical characteristics of the columns are provided in Table S1. The SS (0.6–0.8 mm) was obtained from US Silica Company Inc. (Ottawa, IL, USA). The granular ZVI (0.25–1.19 mm) was obtained from Connelly-GPM Inc. (Chicago, IL, USA), and was washed using 1.2 M HCl acid followed by ultrapure H₂O (Type 1, 18.2 MΩ cm @ 25 °C, generated from a MilliQ A10 water system) before use. The BC (oak hard wood; 0.50–2.36 mm) was obtained from Cowboy Charcoal Co. (Brentwood, TN, USA). The analysis of the hard wood biochar used in this study has been reported previously by Liu et al. (2015). The carbon content of the BC is 99.9%; fourier transform infrared spectroscopy (FTIR) analysis indicates the presence of abundant hydroxyl, aliphatic, quinone, sulfate, and carbonate functional groups on the BC surface. After packing, the columns were wrapped with aluminum foil to minimize exposure to light. The columns were purged with CO₂ (g) for 24 h to displace atmospheric gases in the void pore spaces of the column packing, except for the Column ZVI. CO₂ (g) is more soluble in water than N₂ and O₂, which enhances the saturation of the packing materials. Column ZVI was not purged with CO₂ (g) to avoid the formation of carbonate precipitates, which can cause a decrease in reactivity of the iron (Jeen et al., 2006). The columns were placed in an anaerobic glove box (Coy Laboratory Products Inc., Grass Lake, IL, USA) that contained 5% H₂ and 95% N₂ and were saturated with ultrapure H₂O before the introduction of influent solution.

A concentrated stock solution was prepared that contained 10 mg L⁻¹ of pharmaceutical compounds CBZ, CAF, SMX, 3,4-methylenedioxyamphetamine (MDA), 3,4-methylenedioxymethamphetamine (MDMA), IBU, GEM, and NAP; 100 mg L⁻¹ of artificial sweeteners ACE-K, CYC, SAC, and SCL; and 50–100 mg L⁻¹ of PFOA and PFOS in ultrapure water. About 9% (v/v) methanol (HPLC grade, Sigma-Aldrich) was used in this concentrated stock solution to dissolve the dry powders. The influent solution was prepared by adding 4 mL of

the concentrated stock solution to 4 L of Ar-purged simulated groundwater, resulting in < 0.01% methanol. Simulated groundwater (CaCO₃ saturated water, 0.8–1.0 mM CaCO₃ in H₂O) was used as the influent solution matrix to represent concentrations of dissolved Ca²⁺, HCO₃⁻, and CO₃²⁻ that are often dominant species in natural surface water and groundwater. The final influent solution contained approximately 10 µg L⁻¹ of pharmaceuticals CBZ, CAF, SMX, MDA, MDMA, IBU, GEM, and NAP; 100 µg L⁻¹ of artificial sweeteners ACE-K, CYC, SAC, and SCL; and 50 µg L⁻¹ of PFOA and 20 µg L⁻¹ PFOS for the first 21 pore volumes (PV) of flow. After 21 PV of flow through the columns, the concentration of PFOS in the influent solution was increased to 50–100 µg L⁻¹ to match the influent PFOA concentration; the concentrations of the other target contaminants remained the same.

The experiment was divided into two stages. The influent solution was pumped through the columns from the bottom to the top at a rate of 0.3 pore volume (PV) d⁻¹ during the first stage and at a rate of 0.1 PV d⁻¹ after ~50 PV of flow during the second stage to evaluate the effect of residence time on contaminant removals. The flow rate was set at 0.3 or 0.1 PV d⁻¹ to be representative of average groundwater velocities reported at subsurface-wastewater disposal sites (Benner et al., 1997; Carrara et al., 2008; Robertson et al., 2000). Profile samples were collected four times during the experiments (after 1, 13, 25, and 53 PV of flow) along the length of the columns.

2.2 Sample Collection and Analytical Methods

Water samples were collected from the effluent and profile ports using 125-mL amber glass bottles, except those for PFOA and PFOS analysis which were collected using 30-mL polypropylene bottles. Samples for pH and Eh analysis were not filtered; samples for alkalinity measurements were filtered through 0.45-µm cellulose acetate membranes (Pall Corp.,

Mississauga, ON, Canada). Pharmaceutical samples were filtered through 0.45- μm nylon membranes (Pall Corp., Canada) and collected in 25-mL amber glass vials. Artificial sweetener samples were filtered through 0.2- μm polyvinylidene difluoride (PVDF) membranes (Chromatographic Specialties Inc., Brockville, ON, Canada) and collected in 8-mL polyethylene (HDPE) bottles. Samples for PFOA and PFOS analysis were filtered through 0.45- μm polypropylene membranes (Pall Corp., Canada) and collected in 15-mL HDPE bottles before 36 PV of flow through the columns, but not filtered thereafter. The pH, Eh, and alkalinity measurements were performed immediately after sampling; all other samples were stored at 4 °C until analysis within one month of collection.

The pH was measured using a Ross combination glass electrode (Orion 815600) calibrated using standard pH 7, 4, and 10 buffers before use and checked against pH 7 and 10 buffers between samples. The Eh values were measured using a Pt-billeted Ag-AgCl combination electrode (Orion 9678BNWP). The performance of the Eh probe was checked against A and B solutions (redox/ORP electrode user guide, Thermo Scientific, Canada) between samples. Alkalinity measurements were performed using a Hach digital titrator with bromocresol green/methyl red indicator and 0.08 mol L⁻¹ H₂SO₄.

The analysis of target compounds involved isotope dilution of each compound to track analyte recovery, instrument variability, and matrix suppression during sample analysis. The strategy of using isotope-labelled internal standards and procedures for sample extraction (solid phase extraction, SPE) are summarized in the supplementary information (SI). Analytical procedures for target emerging contaminants using liquid chromatography-electrospray mass spectrometry (LC/MS) or ion chromatography-electrospray mass spectrometry (IC/MS) are

described in the SI, together with calibration curve preparation, quality assurance/quality control (QA/QC) procedures, and method detection limits of target compounds.

3. Results and Discussion

3.1 Column Geochemistry

The average pH of Columns *Control* and *BC* effluents was about 8.3 during the first stage of the experiment, consistent with influent pH values. In response to a decrease in flow rate during the second stage of the experiment, the pH of Column *Control* effluent slightly increased to 8.6, while the pH of Column *BC* effluent decreased to 6.9 (Figure S1). The pH of Column *ZVI* effluent gradually increased from 7.8 at 5 PV to 9.4 until the end of the first stage of the experiment (50 PV), likely due to the reduction of water by *ZVI* ($Fe^0 + 2H_2O \leftrightarrow Fe^{2+} + 2OH^- + H_{2(g)}$) (Wilson, 1923); however, the pH of Column *ZVI* effluent then decreased to 8.6 in the second stage of the experiments (Figure S1). The average pH within Column (*ZVI* + *BC*) and in its effluent was constant at 8.7 through the entire experiment despite the decrease in flow rate. Average Eh values within Columns *Control*, *ZVI*, *BC*, and (*ZVI* + *BC*) were about -410, -450, -395, and -440 mV, respectively (Figure S2), indicating strong reducing conditions were maintained in all of the columns over the course of the experiment. The alkalinity of Columns *Control* and *BC* effluents was consistent with the influent alkalinity, with values decreasing (51–94 mg L⁻¹ as CaCO₃) during the experiment. The alkalinity of Column *ZVI* effluent increased from 14 to 39 mg L⁻¹ (as CaCO₃) during the first stage of the experiment, and then decreased slightly to 27 mg L⁻¹ (as CaCO₃) in the second stage of the experiment. The alkalinity of Column (*ZVI* + *BC*) effluent was slightly lower than for Column *BC* effluent but higher than for Column *ZVI* effluent, likely as a result of the mixed composition of the two reactive media (Figure S1).

3.2 Removal of Pharmaceutical Compounds in Columns

3.2.1 Removal of Pharmaceutical Compounds from Column Effluent

Pharmaceutical compounds CBZ, CAF, MDA, MDMA, IBU, GEM, and NAP were not removed in Column *Control*, with similar influent and effluent concentrations observed ($\sim 9 \mu\text{g L}^{-1}$) (Figures 1 and 2). SMX was not removed in Column *Control* in the early stage of the experiment; however, increasing removal was observed after 14 PV, especially during the second stage of the experiment when the effluent concentration declined to $\sim 0.3 \mu\text{g L}^{-1}$. The removal of SMX in Column *Control* was likely due to biodegradation and sorption of SMX to biofilm as a result of microbial growth during the extended operating period, as reported in other studies (Martínez-Hernández et al., 2016). The concentrations of pharmaceutical compounds in Columns *ZVI*, *BC*, and (*ZVI + BC*) effluents decreased from the average input concentration of ~ 9 to $< 0.25 \mu\text{g L}^{-1}$ throughout the experiment, indicating almost complete removal (97-99%) of the eight target pharmaceuticals (Figures 1 and 2). The decrease in flow rate did not affect the removal of pharmaceutical compounds in Columns *ZVI*, *BC*, and (*ZVI + BC*).

3.2.2 Potential Removal Mechanisms of Pharmaceutical Compounds by ZVI and BC

The target pharmaceutical compounds were classified as acids, bases, and acid/base according to the ionizable functional groups (acid deprotonates/base protonates) in their structure. Each type of pharmaceutical was divided into three groups (neutral, cationic, and anionic compounds) according to the charge of the occurring relevant species in the pH range investigated (7.0–9.5) in this study (Table 1 and Figure S3). CBZ is a base ($-\text{NH}_2$ functional group in its structure) and was primarily in its neutral form ($\text{pH} > \text{p}K_a$) in the pH conditions of this study. CAF, MDA, and MDMA are basic compounds because the N-bearing functional groups in these compounds are protonated in the investigated pH range; they were primarily in their cationic forms (positively

charged, $\text{pH} < \text{their pKas}$). SMX is a zwitterion (with two pKas : 1.7 and 5.6) and contains both acidic ($-\text{NH}-$) and basic ($-\text{NH}_2$) functional groups; SMX predominantly exists as an anionic species (negatively charged) at $\text{pH} > 5.6$. IBU, GEM, and NAP are acidic compounds because their carboxylic groups are deprotonated at pH values above their pKas ; they were primarily in their anionic forms (negatively charged) in this study. The detailed removal mechanisms of target pharmaceuticals by ZVI and BC are summarized in Table S2.

In this study, removals of target pharmaceuticals by ZVI were likely through direct and indirect reduction by ZVI and iron oxides, adsorption or coprecipitation on corrosion products, H bonding, and electrostatic interaction. Removal of pharmaceuticals CAF, MDA, MDMA, SMX, IBU, GEM, and NAP using ZVI alone has not been previously reported; however, König et al. (2016) report that CBZ can be reduced by ZVI through reductive catalytic hydrogenation (H_2 was produced during anaerobic corrosion of ZVI by H_2O) with nine hydrogenation products identified. Reductive degradation of aqueous IBU (10 mg L^{-1}) by ZVI nanoparticles alone has been reported by Machado et al. (2013), with removals of 54–66% observed; similarly, the decreased removal of IBU observed in this study was likely due to passivation (oxidation) of the ZVI surfaces, which limits electron transfer from the core of the ZVI particles to its surface (Li et al., 2006). The corrosion of Fe^0 in natural waters (pH 4–9) produces hydrated iron oxide films on the metal surface (Wilson, 1923), and the $-\text{OH}$ groups (H donors and acceptors) of iron hydroxide can interact with N, $-\text{NH}-$, $-\text{NH}_2$, $=\text{O}$, $-\text{O}-$, $-\text{COOH}$, and OH groups (H donors and acceptors) of target pharmaceuticals through H bonding, which likely enhanced the removal of target pharmaceuticals by ZVI (Table S2). Common products of Fe^0 corrosion and precipitation in dissolved calcium carbonate water (simulated groundwater) are iron hydroxy carbonate [$\text{Fe}_2(\text{OH})_2\text{CO}_3$] and aragonite (CaCO_3), as have been identified by Jeon et al. (2007) in a

previous column experiment conducted under similar geochemical conditions. The iron hydroxy carbonate is likely negatively charged in the pH range of this study (pH 7.9–9.5) (Guilbaud et al., 2013). The electrostatic interaction between negatively charged ZVI and positively charged pharmaceuticals (CAF, MDA, and MDMA) can also contribute to the removal of pharmaceuticals by ZVI.

Removal of organic contaminants by BC is attributed to the strong sorption affinity between organic contaminants and BC through hydrophobic interaction, π - π electron donor-acceptor (EDA) interaction, π - π electron coupling interaction between the graphite moieties of BC and π electron of contaminants, electrostatic interaction, and H-bonding (Inyang and Dickenson, 2015; Zhao et al., 2016). The BC used in this study is likely a π -donor (π -electron rich) due to a high graphitic carbon content (99.9%) (Liu et al., 2015). The π - π EDA interaction likely formed between electron withdrawing functional groups (N, -NH-, -NH₂, C=O, -O-, sulfonamide, heterocyclic ring, and carboxyl groups) in CAF, MDA, MDMA, SMX, IBU, GEM, NAP and the π -electron rich BC (Jung et al., 2013; Zheng et al., 2013). The π - π stacking interaction between the aromatic rings in CBZ, MDA, MDMA, SMX, IBU, GEM, and NAP molecules and the aromatic structure of graphene in the BC also likely enhanced the sorption of these pharmaceuticals by BC. The BC was likely negatively charged at pH 7.0–9.5 (Mukherjee et al., 2011); positively charged pharmaceuticals (CAF, MDA, and MDMA) can adsorb on negatively charged BC through electrostatic interaction. In addition, H bonding and π -H bonding between the functional groups N, -NH-, -NH₂, C=O, and -OH (H electron donor or acceptors) of target pharmaceuticals and the -OH (H electron donor or acceptors) and aromatic π structure of BC (Liu et al., 2015) also likely contributed to sorption of these compounds by BC. Hydrophobic interaction between moderately hydrophobic CBZ ($\log D_{ow}=2.77$) and hydrophobic

BC likely accounted for the sorption of CBZ by BC (Inyang and Dickenson, 2015); however, the hydrophobic interaction between BC and other target hydrophilic pharmaceuticals (low $\log D_{ow}$ values; Table 1) was limited. In addition, CBZ, SMX, MDA, and MDMA may be sorbed to BC through Lewis acid-base interaction; the amino ($-\text{NH}-$ and $-\text{NH}_2$) on the target pharmaceutical molecules act as the Lewis bases and the O-containing groups ($-\text{OH}$, $-\text{CO}-$, and $-\text{CO}_3-$) on the BC act as Lewis acids (Zhao et al., 2016). Effective stabilization or removal of target pharmaceuticals from contaminated soil and water has been reported using BC (Hurtado et al., 2016; Jung et al., 2015).

3.2.3 Removal Rates of Pharmaceutical Compounds within Columns

The removal of pharmaceutical compounds within Columns *ZVI*, *BC*, and (*ZVI + BC*) followed a first-order rate model (Figures 3 and 4) with $R^2 > 0.93$. The removal rates, first-order removal rate constants (k_{obs}), mass normalized rate constants (k_M), and surface area normalized rate constants (k_{SA} , specific reaction rate constant) of target pharmaceuticals are reported by Liu et al. (2020).

Overall, the pharmaceuticals were removed more rapidly in Columns *ZVI* and (*ZVI + BC*) than in Column *BC*. The removal rates of pharmaceuticals within the treatment columns decreased by 67 to 99% over the experimental period. Decreases in the removal rates of pharmaceuticals by *ZVI* may be related to declining reactivity of *ZVI* due to accumulation of secondary precipitates on the *ZVI* surfaces, such as described for treatment of trichloroethylene (TCE) by *ZVI* (Jeen et al., 2007). The decreasing removal of pharmaceuticals by *BC* may be due to in-filling of pores and decreasing sorption sites over time. The removal rates of pharmaceuticals within Columns *ZVI* and (*ZVI+BC*) was in the following order: $\text{SMX} >$

MDMA > MDA > CAF > CBZ > GEM > NAP > IBU (i.e., SMX > cationic compounds > neutral compounds > anionic compounds or N functional group-bearing compounds > carboxylic functional group-bearing compounds). The removal rates of pharmaceuticals within Column *BC* was in the following order: MDMA > MDA > CAF > CBZ > NAP > GEM > SMX > IBU (i.e., cationic compounds > neutral compounds > anionic compounds) (Liu et al., 2020). Overall, removal rates for cationic pharmaceuticals were greater than for neutral and anionic pharmaceuticals within each treatment column independent of the hydrophobicity ($\log D_{ow}$), number of aromatic rings, and number of H acceptors and donors of the compounds. CBZ was the most hydrophobic (high $\log D_{ow}$ value) pharmaceutical considered in this study, but its removal rate was lower than that of the cationic pharmaceuticals (MDMA, MDA, and CAF). Electrostatic interactions were likely more important than other removal mechanisms such as hydrophobic interactions, π - π EDA and stacking interactions, and H bonding for removing target pharmaceuticals.

3.3 Removal of Artificial Sweeteners in Columns

3.3.1 Removal of Artificial Sweeteners from Column Effluent

Artificial sweeteners ACE-K, CYC, SAC, and SCL (input concentration: 90–120 $\mu\text{g L}^{-1}$) were not removed in Column *Control*. About 27 and 14% of input ACE-K ($\sim 100 \mu\text{g L}^{-1}$) was removed in Columns *ZVI* and (*ZVI + BC*), respectively, during the first stage of the experiment; the removal of ACE-K increased to 61% in Column *ZVI* and to 31% in Column (*ZVI + BC*) during the second stage of the experiment as the flow rate decreased from 0.3 to 0.1 PV d^{-1} . No removal of ACE-K was observed in Column *BC* (Figure 5), consistent with poor removal ($\sim 10\%$) of ACE-K reported using powdered activated carbon (PAC) filtration (Mailler et al., 2015). CYC

was not removed in this study. Scheurer et al. (2010) report poor removal of CYC in a GAC filter with 80% breakthrough after 3 d.

Partial removal of SAC was observed in the two columns containing BC, but not Column *ZVI*. The concentration of SAC in the effluents of Columns *BC* and (*ZVI* + *BC*) gradually increased from trace levels of 1.1-7.3 $\mu\text{g L}^{-1}$ before 6 PV to 81.5-85.5 $\mu\text{g L}^{-1}$ at ~50 PV during the first stage of the experiment with higher concentrations of SAC observed in Column (*ZVI* + *BC*) than Column *BC*. The concentration of SAC then slightly decreased to 70.3 $\mu\text{g L}^{-1}$ at 65 PV in Column *BC* effluent and remained at the input concentration in Column (*ZVI* + *BC*) effluent during the second stage of the experiment (Figure 5).

More than 88, 85, and 76% of input SCL ($\sim 110 \mu\text{g L}^{-1}$) was removed in Columns *ZVI*, *BC*, and (*ZVI* + *BC*), respectively. The SCL concentration in Column *ZVI* effluent increased from 2.6 to 9.3 $\mu\text{g L}^{-1}$ in the first stage of the experiment, and then increased further to 13.1 $\mu\text{g L}^{-1}$ at 58 PV in the second stage of the experiment. The removal of SCL in Column *ZVI* was not enhanced by the decrease in flow rate from 0.3 to 0.1 PV d^{-1} ; however, the removal of SCL in Columns *BC* and (*ZVI* + *BC*) was slightly enhanced with decreasing flow rate. The concentration of SCL in Columns *BC* and (*ZVI* + *BC*) effluents respectively increased from 7.4 and 0.9 $\mu\text{g L}^{-1}$ at 10 PV to 17.2 and 28.4 $\mu\text{g L}^{-1}$ at 53 PV in the first stage of the experiment, then slightly decreased to 12.8 and 24.3 $\mu\text{g L}^{-1}$ at 63 PV in the second stage of the experiment (Figure 5). Greater removal (> 99%) of SCL by AC is demonstrated by Minten et al. (2011) compared to the removal of SCL (85–99%) by BC in this study.

3.3.2 Potential Removal Mechanisms of Artificial Sweeteners by *ZVI* and *BC*

Artificial sweeteners ACE-K, CYC, and SAC were predominantly anionic (negatively charged) in the investigated pH range (7.0–9.5) due to dissociation of these compounds at pH values above their pK_{aS} (Table 1 and Figure S3). SCL was mainly in its neutral form ($pH < pK_a$) in this study. The potential removal mechanisms of artificial sweeteners by ZVI and BC are summarized in Table S3. The removal of ACE-K and SCL by ZVI has not been previously reported. The removal of ACE-K by ZVI was likely due to reduction; removal of SCL by ZVI was likely through dechlorination of the chlorine atoms in the SCL molecule by ZVI. In addition, the H bonding between =O and N bearing groups (H acceptors) of ACE-K, –OH groups (H donors and acceptors) of SCL, and –OH groups on the surface of ZVI may also have contributed to removal of ACE-K and SCL by ZVI.

The sorption of SAC by BC is attributed to π – π stacking interaction between the aromatic ring in SAC and aromatic structure of graphene in the BC. The π – π EDA interaction between electron-withdrawing sulfonamide and carbonyl functional groups (π electron acceptors) in SAC and the π -electron-rich BC (π -electron donors) also likely contributed to the sorption of SAC by BC (Inyang and Dickenson, 2015). In addition, the H bonding between the =O and N bearing groups (H acceptors) in the SAC molecule and the –OH (H donors) of BC could also contribute to sorption of SAC by BC. Similarly, Seo et al. (2016) report that the H bonding between the –NH₂ group (H donor) on modified sorbent and =O (H acceptor) in the SAC molecule contributes to the adsorptive removal of SAC by urea-modified metal–organic frameworks. The sorption of SCL by BC was likely through H bonding. Sucralose contains –OH, which might be attracted to the –CO– and –OH in BC through H bonding. Hydrophobic interactions and electrostatic interactions between SAC and SCL (hydrophilic and neutral or negatively charged) and BC

(hydrophobic and negatively charged) were assumed to have been limited in this study (Table S3).

3.3.3 Removal Rates of Artificial Sweeteners within Columns

The removal of artificial sweeteners followed first- or zero-order rate models or followed a first-order rate in the early stage of the experiment followed by a zero-order rate in the late stage of the experiment (Figure 6). The first- and zero-order removal rates, removal rate constants (k_{obs}), mass normalized rate constants (k_M), and surface area normalized rate constants (k_{SA} , specific reaction rate constant) are reported by Liu et al. (2020).

ACE-K was removed more rapidly within Column *ZVI* (first-order model) than Column (*ZVI+BC*) (zero-order model). The average removal rate of ACE by *ZVI* in this study was much greater than observed by direct photolysis of ACE-K at pH 4 in deionized water with a rate constant of 0.036 d^{-1} (Gan et al., 2014). The removal rate of SAC within the three treatment columns was in the following order: $BC > (ZVI + BC) > ZVI$. The removal rate of SCL within the three treatment columns occurred in the order $ZVI > (ZVI + BC) > BC$ before 13 PV and then $BC = (ZVI + BC) > ZVI$ after 13 PV (Figure 6) (Liu et al., 2020). This decrease in SCL removal rates by *ZVI* was likely due to the declining reactivity of *ZVI*. The removal rates of ACE-K, SAC, and SCL within treatment columns were lower than those observed using advanced oxidation technologies (Sharma et al., 2014; Toth et al., 2012).

Overall, adding *ZVI* to *BC* did not enhance the removal of artificial sweeteners ACE-K, CYC, SAC, and SCL; artificial sweeteners were less effectively removed in Column (*ZVI + BC*) than in either Column *ZVI* or *BC*. The removal rate of four artificial sweeteners was $SCL > ACE-$

K > SAC > CYC (no removal) within Column ZVI and SCL > SAC > ACE-K and CYC (no removals) within the column containing BC.

3.4 Removal of PFOA and PFOS in Columns

3.4.1 Removal of PFOA and PFOS from Column Effluent

PFOA and PFOS were persistent and not removed in the Column *Control*. More than 89% of input PFOA ($\sim 45 \mu\text{g L}^{-1}$) was removed in Columns ZVI, BC, and (ZVI + BC) early in the first stage of the experiment (< 10 PV); the removal efficiency then greatly decreased in all three treatment columns over the remainder of the experiment. The concentration of PFOA in Column ZVI effluent was $< 0.5 \mu\text{g L}^{-1}$ before 10 PV with a removal of 99%, then rapidly increased to $51.4 \mu\text{g L}^{-1}$ (10 to 25% higher than the input PFOA) at 18 PV until the end of the first stage of the experiment. The concentration of PFOA then gradually decreased to the influent PFOA level during the second stage of the experiment. More than 90% of the input PFOA was removed from Columns BC and (ZVI + BC), from an influent concentration of $44.6 \mu\text{g L}^{-1}$ to effluent concentrations of $< 5 \mu\text{g L}^{-1}$, within the first 6 PV in the first stage of the experiment. However, the effluent PFOA concentration in both columns gradually increased to influent concentrations, with much greater removals observed in Column BC than in Column (ZVI + BC). In addition, an effluent PFOA concentration ($\sim 55.4 \mu\text{g L}^{-1}$) greater than the influent concentration was observed in Column (ZVI + BC), similar to Column ZVI. The removal of PFOA in Columns BC and (ZVI + BC) was slightly enhanced at lower flow rates; however, breakthrough of PFOA in both columns was observed by the end of the experiment with effluent concentrations of $50.7 \mu\text{g L}^{-1}$ in Column BC and $45 \mu\text{g L}^{-1}$ in Column (ZVI + BC) (Figure 7).

Columns containing BC removed about 49–98% of input PFOS ($24.0\text{--}89.6\ \mu\text{g L}^{-1}$) over the experimental period; less was removed by Column *ZVI* (Figure 7). More than 81% of input PFOS ($24.0\text{--}82.6\ \mu\text{g L}^{-1}$) was removed in Column *ZVI* before 37 PV during the first stage of the experiment; however, as the average input PFOS concentration increased from 47.5 to $82.9\ \mu\text{g L}^{-1}$ during over the course of 34 to 50 PV, the concentration of PFOS in Column *ZVI* effluent rapidly increased from 2.23 to $51.2\ \mu\text{g L}^{-1}$ with removals decreased to 25–46% by the end of first experimental stage. The concentration of PFOS in Column *ZVI* effluent followed the same trend as the influent PFOS, with relatively lower removals of 11–49% during the second stage of the experiment (Figure 7). More than 82% of input PFOS (which varied from 24.0 to $89.6\ \mu\text{g L}^{-1}$) was removed in Column *BC* throughout the experiment with effluent concentrations $< 8.6\ \mu\text{g L}^{-1}$ and removal of up to 99%, except for 13–21 PV with removals of 63–94%. Relatively less removal of PFOS was observed in Column (*ZVI* + *BC*) compared to Column *BC*. Similarly, low concentrations of PFOS ($< 6.07\ \mu\text{g L}^{-1}$) were observed in the Column (*ZVI* + *BC*) effluent before 41 PV with removal $> 88\%$, except for 15–22 PV with smaller removals of 57–95%. As the average input PFOS concentration increased from 49.0 to $84.7\ \mu\text{g L}^{-1}$ at ~ 40 PV, the effluent PFOS concentration in Column (*ZVI* + *BC*) then increased from 6.07 to $19.2\ \mu\text{g L}^{-1}$ and remained consistent at $\sim 20\ \mu\text{g L}^{-1}$ with relatively smaller removals of 56–79% through the remainder of the experiment (Figure 7). Overall, PFOA (up to 89%) and PFOS (up to 99%) were removed more effectively by high carbon content (99%) BC in this study compared to a previous study. Specifically, Kupryianchyk et al. (2016) report little or no removal of PFOA and PFOS from the top 20 cm of soils at a fire fighting training site contaminated with PFASs; this is attributed to the low C content (19–53%) of their biochars.

3.4.2 Potential Removal Mechanisms of PFOA and PFOS by ZVI and BC

PFOA and PFOS are acidic compounds that deprotonate and exist primarily in their anionic forms (negatively charged) in the pH range of this study ($\text{pH} > \text{pKas}$; Table 1). Removal of PFOA and PFOS by ZVI during the early stage (before 18 PV) of the experiment was likely due to electrostatic interactions, H bonding, and ion-dipole interactions; however, electrostatic interactions were limited after 18 PV through Column ZVI. The pH of pore water in Column ZVI ranged from 7.1 to 8.2 before 18 PV (Figure S1); Fe(III) (oxy)hydroxide surfaces are positively charged at $\text{pH} < 8.3$ (Parks, 1965), which may have promoted sorption of negatively charged PFOA and PFOS through electrostatic interactions. Similarly, the sorption of PFOA and PFOS by ZVI oxidation products (iron oxides and hydroxides) through electrostatic interactions in a low pH (3.0–6.0) aqueous solution has been reported (Gao and Chorover, 2012). However, the pH of pore water in Column ZVI was > 8.3 after 18 PV, which resulted in negatively charged iron hydroxides and led to a reduction in electrostatic interactions between the iron hydroxide surface and negatively charged PFOA and PFOS. This pH-induced decrease of electrostatic interactions possibly resulted in the desorption of PFOA from ZVI, resulting in the higher concentration of PFOA (10–25%) in Column ZVI effluent compared to the influent PFOA (18–50 PV) (Figure 7).

The H bonding between PFOA/PFOS and ZVI likely occurred between the –OH groups (H donors) on iron hydroxide surfaces and the carboxylic (–COO⁻, 2O as 2H acceptors) and sulfonic (–SO₃⁻, 3O as 3H acceptors) groups of PFOA and PFOS. The H bonding between PFOS (3H acceptors) and ZVI was likely greater than between PFOA (2H acceptors) and ZVI; this may account for the greater removal of PFOS by ZVI than PFOA (Table S4). The anionic PFOA and PFOS molecules can also develop ion-dipole interactions with the polar –OH functional groups (dipole) on the ZVI surface (Punyapalukul et al., 2013). In addition, the formation of Fe-

carboxylate complexes from the ferric Fe hydroxide on the surface of ZVI and the carboxylic group in PFOA may also contribute to sorption of PFOA by ZVI (Gao and Chorover, 2012). Park et al. (2018) also reported removal of PFOS by nano-ZVI through adsorption and complexation with Fe hydroxide.

Fluoride, the indicative by-product of defluorination, was not observed in the treated effluent of any column in this study; this is attributed to a lack of defluorination reactions, analytical limitations, or the removal of F^- by the reactive media. Sorption of F^- by iron hydroxide (Sujana et al., 2009) and biochars (Guan et al., 2015) has been reported. In addition, Ca^{2+} in the simulated groundwater used in this study may have reacted with F^- to form CaF_2 precipitates, therefore also removing F^- from the column effluent and pore water. Therefore, reductive defluorination of PFOA and PFOS by ZVI cannot be confirmed in this study. However, reductive defluorination of PFOA and PFOS is demonstrated by Arvaniti et al. (2015) using Mg-aminoclay modified nanoscale ZVI.

Removal of PFOA and PFOS by BC is attributed to hydrophobic interactions between the hydrophobic perfluoroalkyl tail and hydrophobic surface of BC (Du et al., 2014). In addition, H bonding and ion-dipole interactions may also contribute to the removal of PFOA and PFOS by BC. Greater removals of PFOS than PFOA by BC are attributed to the stronger hydrophobic interaction between PFOS and BC. PFOA and PFOS have the same carbon chain length (C8); however, PFOS contains two additional C-F bonds, which leads to stronger hydrophobicity of PFOS than PFOA (Higgins and Luthy, 2006). Similarly, H bonding between the $-OH$ groups (H donors) in BC and the $-SO_3^-$ group (3H acceptors) in PFOS was greater than the H bonding between the $-OH$ groups in BC and the $-COO^-$ group (2H acceptors) in PFOA. This stronger H bonding between BC and PFOS may have contributed to the stronger sorption of PFOS than

PFOA by BC (Gao and Chorover, 2012). A relatively weak ion-dipole interaction between the –OH dipole groups in BC and anionic PFOA and PFOS molecules can also contribute to the sorption of PFOA and PFOS to BC (Du et al., 2014; Karoyo and Wilson, 2013). In addition, the Ca^{2+} present in simulated groundwater in this study has been reported to enhance the sorption of PFOA and PFOS to adsorbents due to the formation of a cation bridge between Ca^{2+} and negatively charged carboxyl and sulfonate groups (Wang and Shih, 2011). Electrostatic interaction between negatively charged PFOA and PFOS and negatively charged ZVI and BC was likely limited in this study.

3.4.3 Removal Rates of PFOA and PFOS within Columns

The removal of PFOA and PFOS followed first-order, zero-order, or first-order (early stage of the experiment) followed by zero-order (late stage of the experiment) rates (Figure 8). The removal rates, removal rate constants (k_{obs}), mass normalized rate constants (k_M), and surface area normalized rate constants (k_{SA} , specific reaction rate constant) are reported by Liu et al. (2020). The removal rate of PFOA occurred in columns in the following order: $BC > (ZVI + BC) > ZVI$. The removal rate of PFOS occurred in columns in the order $(ZVI + BC) > BC > ZVI$ during the first stage of the experiment and $BC > (ZVI + BC) > ZVI$ during the second stage of the experiment (Figure 8). Overall, PFOA and PFOS were removed more rapidly within the two columns containing BC than only ZVI.

The decreasing removal rates of PFOA and PFOS by the columns containing BC were likely due to the competitive sorption between PFASs and other organic contaminants pharmaceuticals, and artificial sweeteners, as previously reported (Yu et al., 2012). In addition, Du et al. (2014) demonstrate that the adsorbed negatively charged PFAS molecules on the

sorbents produce a repulsive force which prevents further adsorption of negatively charged PFASs. This repulsive interaction on the surface of BC also likely decreased the sorption efficiency of PFOA and PFOS by BC over time. The removal rates of PFOA and PFOS by ZVI and BC were slower than reported using the iron containing material hematite (Gao and Chorover, 2012) and carbonaceous sorbent GAC (Zhang et al., 2016).

4. Conclusions

Simultaneous removal of 13 emerging contaminants, specifically pharmaceutical compounds (CBZ, CAF, MDA, MDMA, SMX, IBU, GEM, and NAP with removals > 97%), artificial sweeteners (ACE-K, SAC, and SCL with partial removals), and perfluoroalkyl substances (PFOA and PFOS with partial removals), was observed in a passive treatment system (four columns) containing reactive media composed of zero-valent iron, biochar, and a mixture thereof. Eight pharmaceuticals were more rapidly and completely removed in the columns containing ZVI than only BC. In general, removal rates of pharmaceuticals within the three treatment columns followed a predictable pattern: SMX (in Column ZVI but not in the columns containing BC) > cationic compounds (MDMA, MDA, and CAF) > neutral compound (CBZ) > anionic compounds (NAP, GEM, and IBU). The removal rates of artificial sweeteners within the treatment columns occurred in the order SCL > ACE-K and SAC > CYC (no removal). Unlike pharmaceuticals, greater and relatively more rapid removals of PFOA and PFOS were observed in the columns containing BC than only ZVI; PFOS was more effectively removed than PFOA. Overall, target pharmaceuticals, artificial sweeteners (except for CYC with no removal), and perfluoroalkyl substances were better removed using the combination of ZVI and BC than either ZVI or BC alone. These results suggest that the reactive mixture of ZVI and BC has the potential to be an effective combination for use in large-scale field applications such as *in situ* reactors and

permeable reactive barriers (PRBs) for remediation of emerging contaminants. These materials are relatively low cost and, when combined, show considerable reactivity for ubiquitous trace organic emerging contaminants present in wastewater. However, more extensive study is required when the reactive mixture is applied to remove emerging contaminants from different wastewater streams, as the complex matrix of the wastewater such as DOC content and ionic strength may influence the removal efficiency. In addition, the identification of degradation products of target emerging contaminants by reactive media should be considered in future studies.

Acknowledgement

Funding for this research was provided by a Discovery Grant awarded to C. Ptacek by the Natural Sciences and Engineering Research Council of Canada.

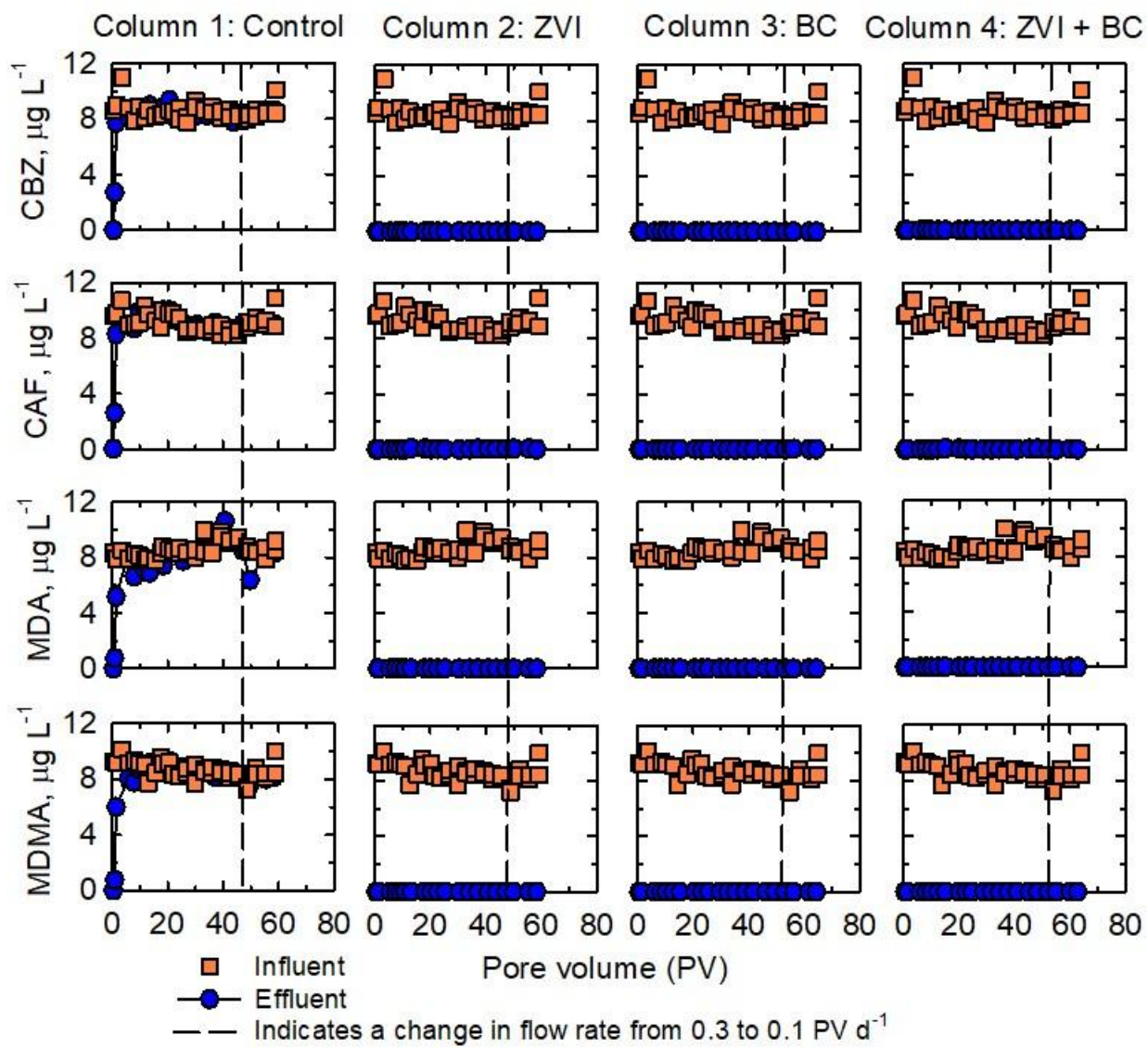


Figure 1 Concentrations of neutral pharmaceutical carbamazepine (CBZ) and cationic pharmaceuticals caffeine (CAF), 3,4-methylenedioxyamphetamine (MDA), and 3,4-methylenedioxymethamphetamine (MDMA) as a function of pore volumes (PV) in effluent from the control column and columns containing zero-valent Fe (ZVI), biochar (BC), and a mixture thereof; dashed lines indicate a decrease in flow rate in each column, dividing the experiment into two stages.

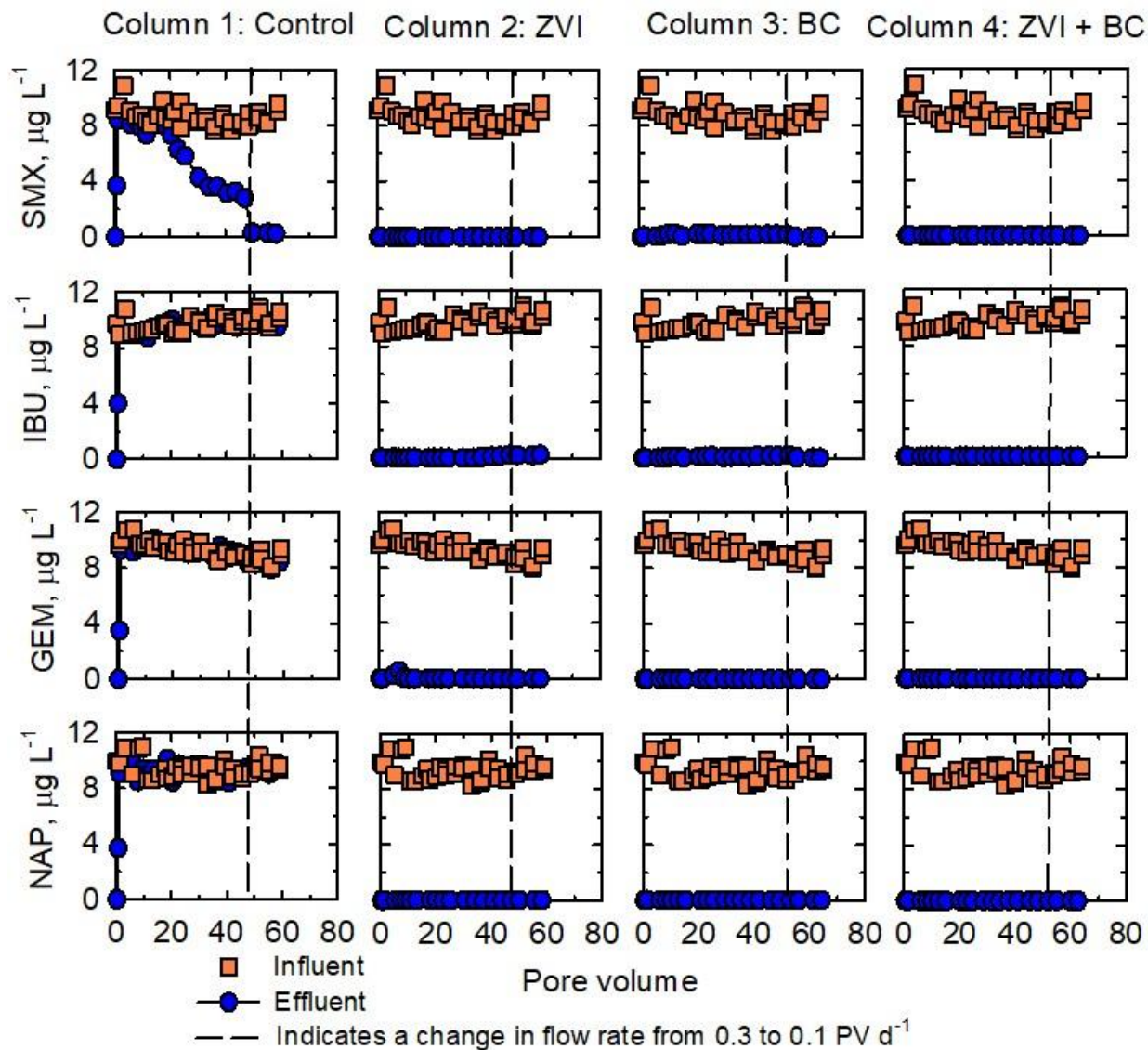


Figure 2 Concentrations of anionic pharmaceuticals sulfamethoxazole (SMX), ibuprofen (IBU), gemfibrozil (GEM), and naproxen (NAP) as a function of pore volumes (PV) in effluent from the control column and columns containing zero-valent Fe (ZVI), biochar (BC), and a mixture thereof; dashed lines indicate a decrease in flow rate in each column, dividing the experiment into two stages.

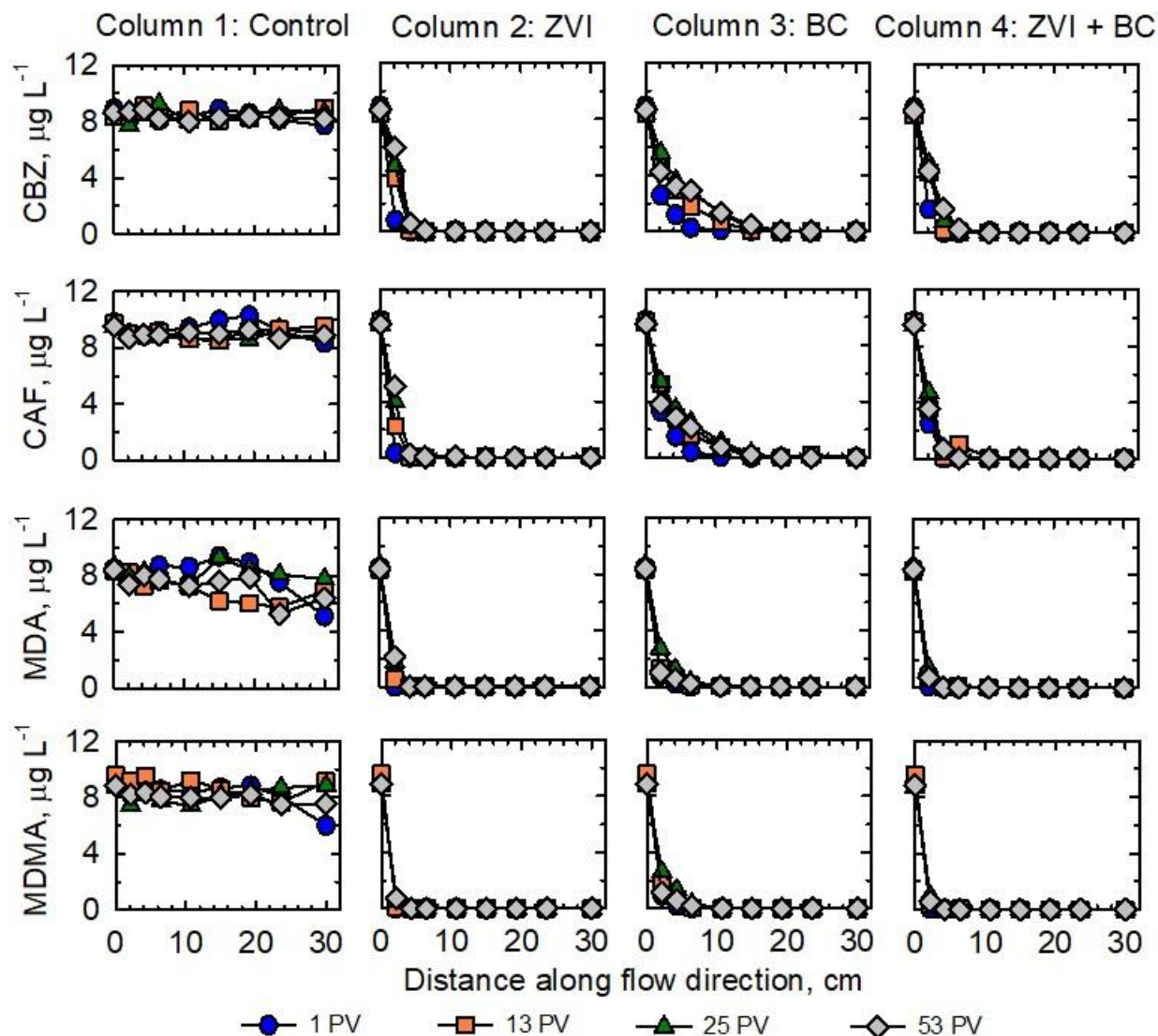


Figure 3 Concentrations of neutral pharmaceutical carbamazepine (CBZ) and cationic pharmaceuticals caffeine (CAF), 3,4-methylenedioxyamphetamine (MDA), and 3,4-methylenedioxymethamphetamine (MDMA) as a function of distance along flow direction within the control column and columns containing zero-valent Fe (ZVI), biochar (BC), and a mixture thereof. Blue circles, orange squares, and green triangles represent data collected during the first stage of the experiment (flow rate = 0.3 PV d^{-1}), while grey diamonds represent data collected during the second stage of the experiment (flow rate = 0.1 PV d^{-1}), given in terms of pore volumes (PV).

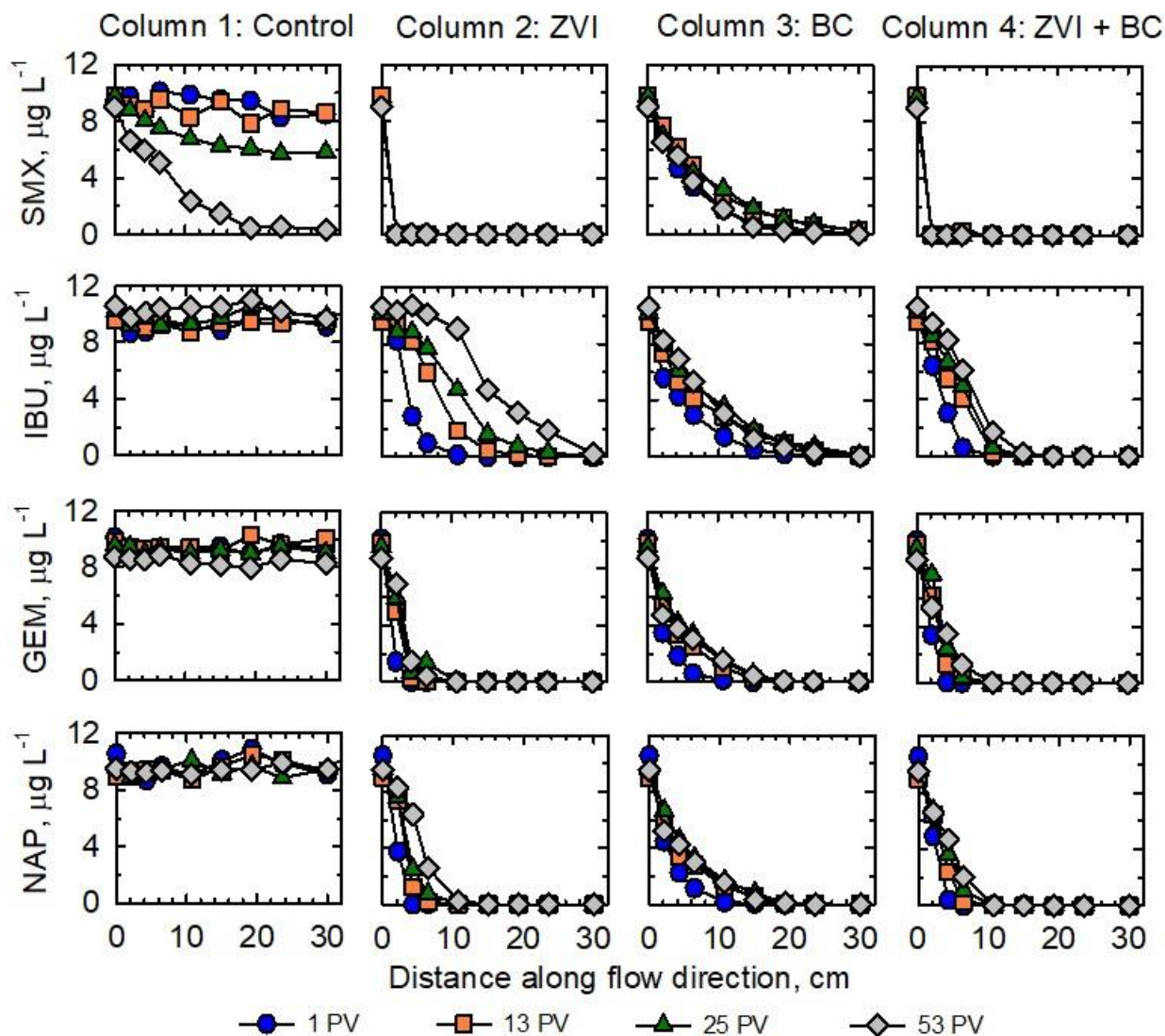


Figure 4 Concentrations of anionic pharmaceuticals sulfamethoxazole (SMX), ibuprofen (IBU), gemfibrozil (GEM), and naproxen (NAP) as a function of distance along flow direction within the control column and columns containing zero-valent Fe (ZVI), biochar (BC), and a mixture thereof. Blue circles, orange squares, and green triangles represent data collected during the first stage of the experiment (flow rate = 0.3 PV d⁻¹), while grey diamonds represent data collected during the second stage of the experiment (flow rate = 0.1 PV d⁻¹), given in terms of pore volumes (PV).

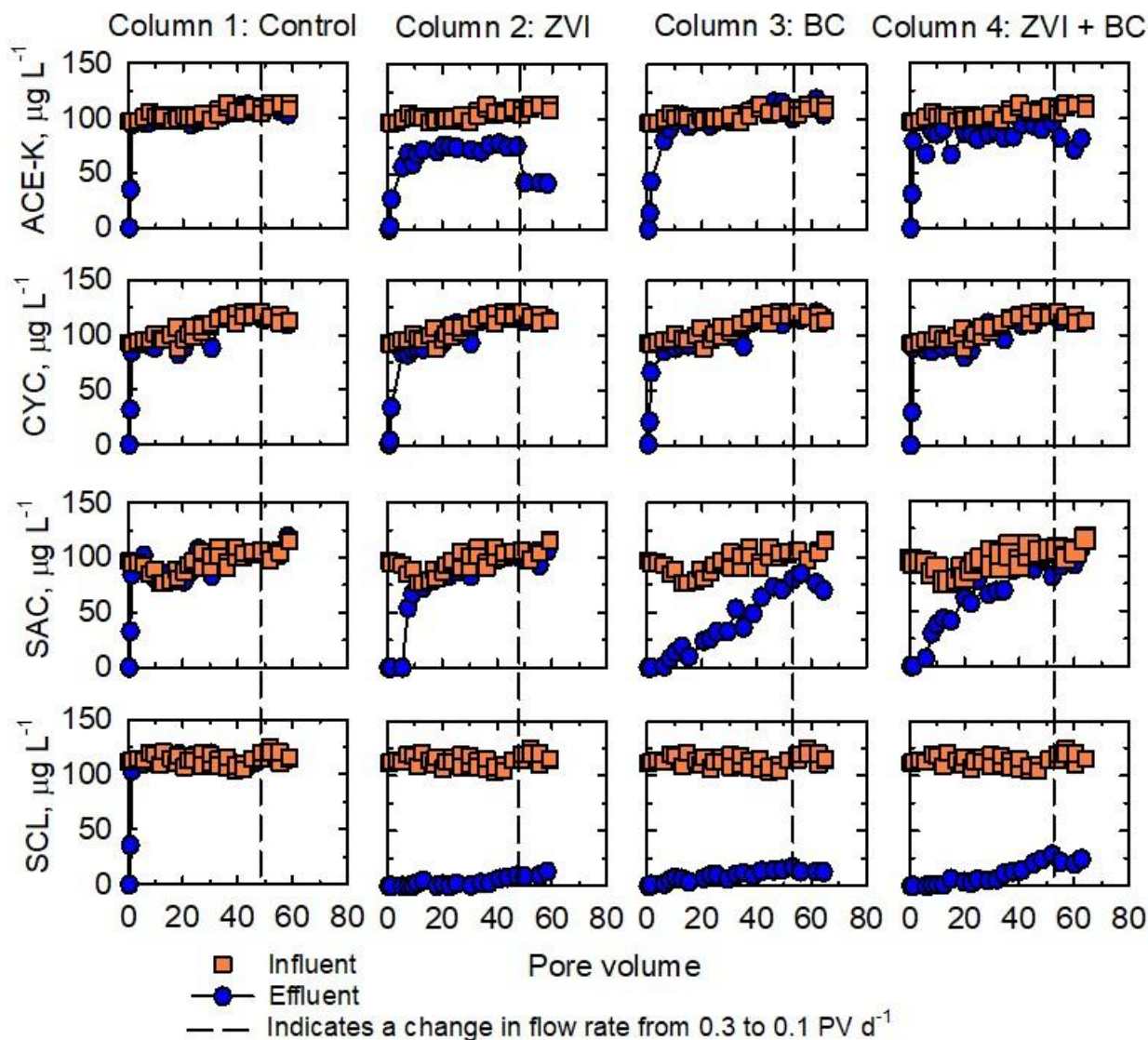


Figure 5 Concentrations of acesulfame-K (ACE-K), cyclamate (CYC), saccharine (SAC), and sucralose (SCL) as a function of pore volumes (PV) in effluent from the control column and columns containing zero-valent Fe (ZVI), biochar (BC), and a mixture thereof; dashed lines indicate a decrease in flow rate in each column, dividing the experiment into two stages.

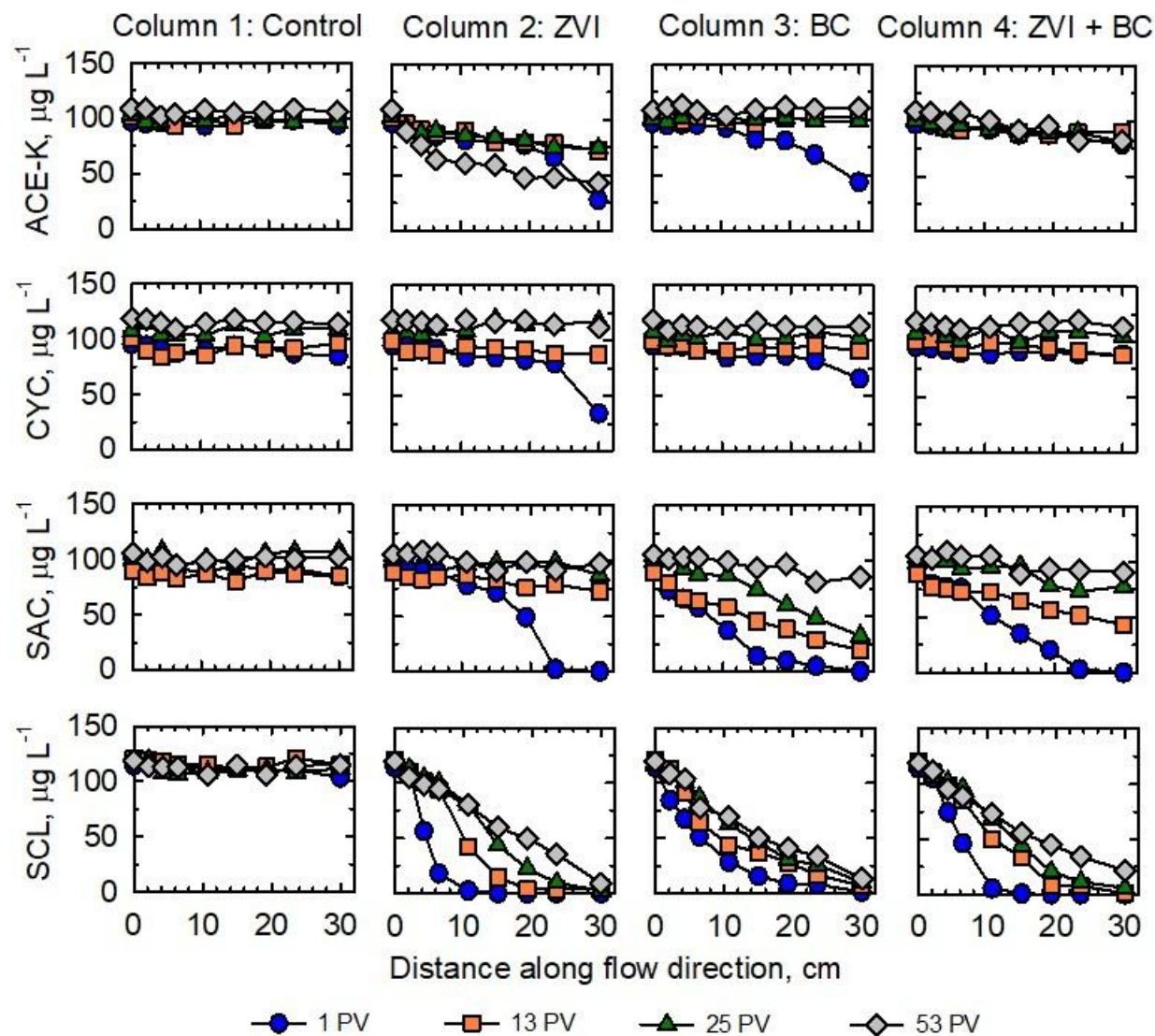


Figure 6 Concentrations of acesulfame-K (ACE-K), cyclamate (CYC), saccharine (SAC), and sucralose (SCL) as a function of distance along flow direction within the control column and columns containing zero-valent Fe (ZVI), biochar (BC), and a mixture thereof. Blue circles, orange squares, and green triangles represent data collected during the first stage of the experiment (flow rate = 0.3 PV d^{-1}), while grey diamonds represent data collected during the second stage of the experiment (flow rate = 0.1 PV d^{-1}), given in terms of pore volumes (PV).

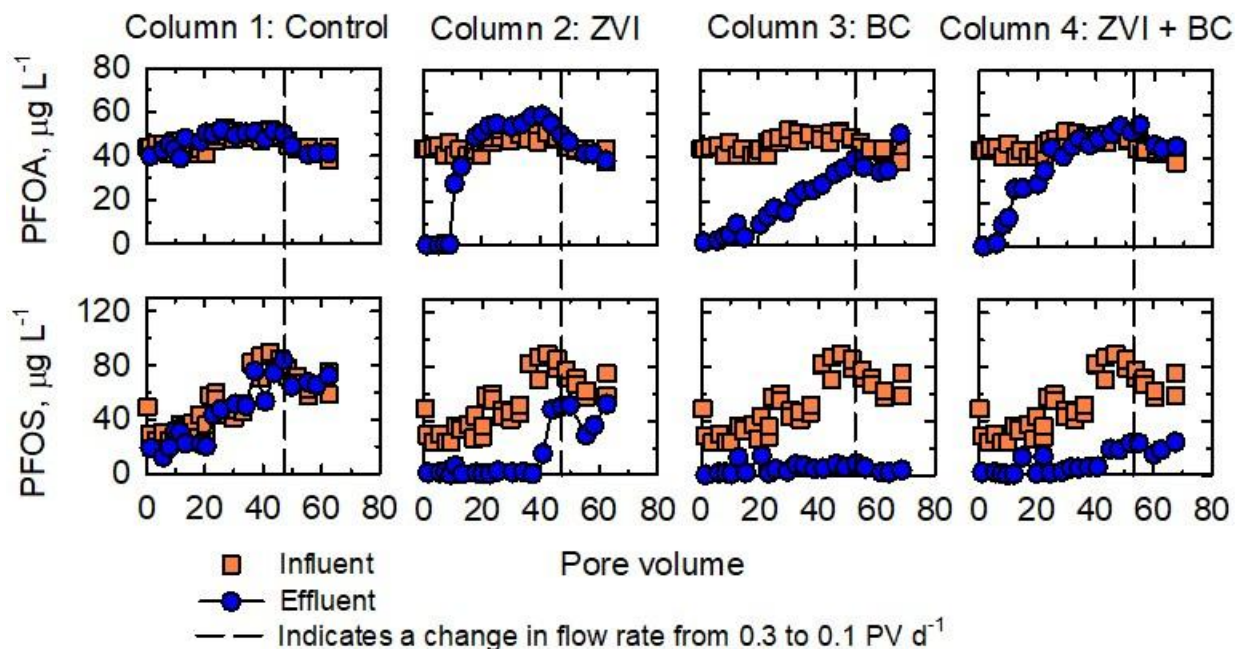


Figure 7 Concentrations of perfluorooctanoic acid (PFOA) and perfluorooctane sulfonic acid (PFOS) as a function of pore volumes (PV) in effluent from the control column and columns containing zero-valent Fe (ZVI), biochar (BC), and a mixture thereof; dashed lines indicate a decrease in flow rate in each column, dividing the experiment into two stages.

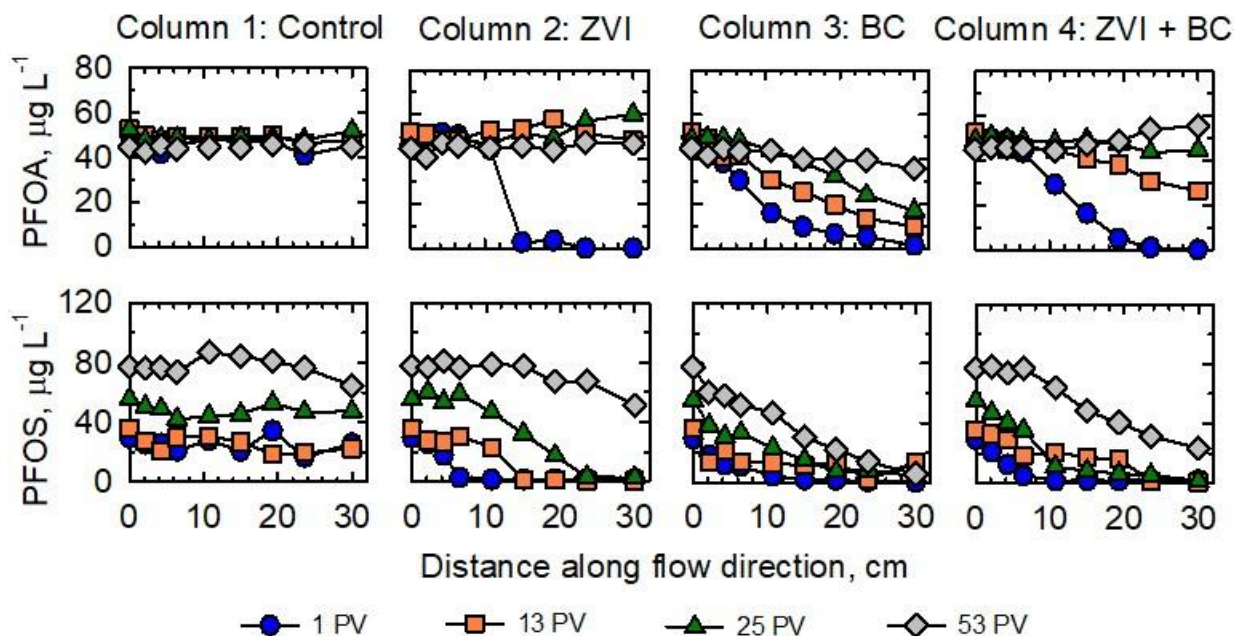


Figure 8 Concentrations of perfluorooctanoic acid (PFOA) and perfluorooctane sulfonic acid (PFOS) as a function of distance along flow direction within the control column and columns containing zero-valent Fe (ZVI), biochar (BC), and both. Blue circles, orange squares, and green triangles represent data collected during the first stage of the experiment (flow rate = 0.3 PV d^{-1}), while grey diamonds represent data collected during the second stage of the experiment (flow rate = 0.1 PV d^{-1}), given in terms of pore volumes (PV).

References

- Ahmed, M.B., Zhou, J.L., Ngo, H.H., Guo, W., Thomaidis, N.S., Xu, J., 2016. Progress in the biological and chemical treatment technologies for emerging contaminant removal from wastewater: A critical review. *J. Hazard. Mater.* 323, Part A, 274–298.
- Ahrens, L., 2011. Polyfluoroalkyl compounds in the aquatic environment: A review of their occurrence and fate. *J. Environ. Monit.* 13(1), 20-31.
- Anderson, R.H., Long, G.C., Porter, R.C., Anderson, J.K., 2016. Occurrence of select perfluoroalkyl substances at U.S. Air Force aqueous film-forming foam release sites other than fire-training areas: Field-validation of critical fate and transport properties. *Chemosphere.* 150, 678-685.
- Appleman, T.D., Dickenson, E.R.V., Bellona, C., Higgins, C.P., 2013. Nanofiltration and granular activated carbon treatment of perfluoroalkyl acids. *J. Hazard. Mater.* 260, 740-746.
- Arvaniti, O.S., Hwang, Y., Andersen, H.R., Stasinakis, A.S., Thomaidis, N.S., Aloupi, M., 2015. Reductive degradation of perfluorinated compounds in water using Mg-aminoclay coated nanoscale zero valent iron. *Chem. Eng. J.* 262, 133-139.
- Benner, S.G., Blowes, D.W., Gould, W.D., Herbert Jr, R.B., Ptacek, C.J., 1999. Geochemistry of a permeable reactive barrier for metals and acid mine drainage. *Environ. Sci. Technol.* 33(16), 2793-2799.
- Benner, S.G., Blowes, D.W., Ptacek, C.J., 1997. A full-scale porous reactive wall for prevention of acid mine drainage. *Ground Water Monit. R.* 17(4), 99-107.
- Bo, L., Shengen, Z., Chang, C.C., Zhanfeng, D., Hongxiang, L., 2015. Emerging pollutants-Part II: Treatment. *Water Environ. Res.* 87(10), 1873-1900.
- Carrara, C., Ptacek, C.J., Robertson, W.D., Blowes, D.W., Moncur, M.C., Sverko, E., Backus, S., 2008. Fate of pharmaceutical and trace organic compounds in three septic system plumes, Ontario, Canada. *Environ. Sci. Technol.* 42(8), 2805-2811.
- Ding, G., Peijnenburg, W.J.G.M., 2013. Physicochemical properties and aquatic toxicity of poly- and perfluorinated compounds. *Crit. Rev. Environ. Sci. Technol.* 43(6), 598-678.
- Du, Z., Deng, S., Bei, Y., Huang, Q., Wang, B., Huang, J., Yu, G., 2014. Adsorption behavior and mechanism of perfluorinated compounds on various adsorbents-A review. *J. Hazard. Mater.* 274, 443-454.
- Gan, Z., Sun, H., Wang, R., Hu, H., Zhang, P., Ren, X., 2014. Transformation of acesulfame in water under natural sunlight: Joint effect of photolysis and biodegradation. *Water Res.* 64, 113-122.
- Gao, X., Chorover, J., 2012. Adsorption of perfluorooctanoic acid and perfluorooctanesulfonic acid to iron oxide surfaces as studied by flow-through ATR-FTIR spectroscopy. *Envir. Chem.* 9(2), 148-157.
- Gillham, R.W., O'Hannesin, S.F., 1994. Enhanced Degradation of Halogenated Aliphatics by Zero - Valent Iron. *Groundwater.* 32(6), 958-967.
- Guan, X., Zhou, J., Ma, N., Chen, X., Gao, J., Zhang, R., 2015. Studies on modified conditions of biochar and the mechanism for fluoride removal. *Desalin. Water Treat.* 55(2), 440-447.
- Guilbaud, R., White, M.L., Poulton, S.W., 2013. Surface charge and growth of sulphate and carbonate green rust in aqueous media. *Geochim. Cosmochim. Acta.* 108, 141-153.
- Higgins, C.P., Luthy, R.G., 2006. Sorption of perfluorinated surfactants on sediments. *Environ. Sci. Technol.* 40(23), 7251-7256.

- Hori, H., Nagaoka, Y., Yamamoto, A., Sano, T., Yamashita, N., Taniyasu, S., Kutsuna, S., Osaka, I., Arakawa, R., 2006. Efficient decomposition of environmentally persistent perfluorooctanesulfonate and related fluorochemicals using zerovalent iron in subcritical water. *Environ. Sci. Technol.* 40(3), 1049-1054.
- Hurtado, C., Cañameras, N., Domínguez, C., Price, G.W., Comas, J., Bayona, J.M., 2016. Effect of soil biochar concentration on the mitigation of emerging organic contaminant uptake in lettuce. *J. Hazard. Mater.* 323, Part A, 386–393.
- Inyang, M., Dickenson, E., 2015. The potential role of biochar in the removal of organic and microbial contaminants from potable and reuse water: A review. *Chemosphere.* 134, 232-240.
- James, C.A., Miller-Schulze, J.P., Ultican, S., Gipe, A.D., Baker, J.E., 2016. Evaluating Contaminants of Emerging Concern as tracers of wastewater from septic systems. *Water Res.* 101, 241-251.
- Jeen, S.W., Gillham, R.W., Blowes, D.W., 2006. Effects of carbonate precipitates on long-term performance of granular iron for reductive dechlorination of TCE. *Environ. Sci. Technol.* 40(20), 6432-6437.
- Jeen, S.W., Jambor, J.L., Blowes, D.W., Gillham, R.W., 2007. Precipitates on granular iron in solutions containing calcium carbonate with trichloroethene and hexavalent chromium. *Environ. Sci. Technol.* 41(6), 1989-1994.
- Jeen, S.W., Yang, Y., Gui, L., Gillham, R.W., 2013. Treatment of trichloroethene and hexavalent chromium by granular iron in the presence of dissolved CaCO_3 . *J. Contam. Hydrol.* 144, 108-121.
- Jung, C., Boateng, L.K., Flora, J.R.V., Oh, J., Braswell, M.C., Son, A., Yoon, Y., 2015. Competitive adsorption of selected non-steroidal anti-inflammatory drugs on activated biochars: Experimental and molecular modeling study. *Chem. Eng. J.* 264, 1-9.
- Jung, C., Park, J., Lim, K.H., Park, S., Heo, J., Her, N., Oh, J., Yun, S., Yoon, Y., 2013. Adsorption of selected endocrine disrupting compounds and pharmaceuticals on activated biochars. *J. Hazard. Mater.* 263, 702-710.
- Karoyo, A.H., Wilson, L.D., 2013. Tunable macromolecular-based materials for the adsorption of perfluorooctanoic and octanoic acid anions. *J. Colloid Interface Sci.* 402, 196-203.
- König, A., Weidauer, C., Seiwert, B., Reemtsma, T., Unger, T., Jekel, M., 2016. Reductive transformation of carbamazepine by abiotic and biotic processes. *Water Res.* 101, 272-280.
- Kupryianchyk, D., Hale, S.E., Breedveld, G.D., Cornelissen, G., 2016. Treatment of sites contaminated with perfluorinated compounds using biochar amendment. *Chemosphere.* 142, 35-40.
- Li, X.Q., Elliott, D.W., Zhang, W.X., 2006. Zero-valent iron nanoparticles for abatement of environmental pollutants: Materials and engineering aspects. *Crit. Rev. Solid State Mater. Sci.* 31(4), 111-122.
- Liu, P., Ptacek, C.J., Blowes, D.W., Berti, W.R., Landis, R.C., 2015. Aqueous leaching of organic acids and dissolved organic carbon from various biochars prepared at different temperatures. *J. Environ. Qual.* 44(2), 684-695.
- Liu, X., Cao, Z., Yuan, Z., Zhang, J., Guo, X., Yang, Y., He, F., Zhao, Y., Xu, J., 2018. Insight into the kinetics and mechanism of removal of aqueous chlorinated nitroaromatic antibiotic chloramphenicol by nanoscale zero-valent iron. *Chem. Eng. J.* 334, 508-518.
- Liu, Y.Y., Blowes, D.W., Groza, L., Sabourin, M.J., Ptacek, C.J., 2014a. Acesulfame-K and

- pharmaceuticals as co-tracers of municipal wastewater in a receiving river. *Environ. Sci.: Processes Impacts*. 16(12), 2789-2795.
- Liu, Y.Y., Blowes, D.W., Ptacek, C.J., 2020. Data on removal kinetics of pharmaceutical compounds, artificial sweeteners, and perfluoroalkyl substances from water using a passive treatment system containing zero-valent iron and biochar. *Data in Brief*. Accepted.
- Liu, Y.Y., Ptacek, C.J., Blowes, D.W., 2014b. Treatment of dissolved perchlorate, nitrate, and sulfate using zero-valent iron and organic carbon. *J. Environ. Qual.* 43(3), 842-850.
- Machado, S., Stawiński, W., Slonina, P., Pinto, A.R., Grosso, J.P., Nouws, H.P.A., Albergaria, J.T., Delerue-Matos, C., 2013. Application of green zero-valent iron nanoparticles to the remediation of soils contaminated with ibuprofen. *Sci. Total Environ.* 461-462, 323-329.
- Mailler, R., Gasperi, J., Coquet, Y., Deshayes, S., Zedek, S., Cren-Olivé, C., Cartiser, N., Eudes, V., Bressy, A., Caupos, E., Moilleron, R., Chebbo, G., Rocher, V., 2015. Study of a large scale powdered activated carbon pilot: Removals of a wide range of emerging and priority micropollutants from wastewater treatment plant effluents. *Water Res.* 72, 315-330.
- Martínez-Hernández, V., Meffe, R., Herrera López, S., de Bustamante, I., 2016. The role of sorption and biodegradation in the removal of acetaminophen, carbamazepine, caffeine, naproxen and sulfamethoxazole during soil contact: A kinetics study. *Sci. Total Environ.* 559, 232-241.
- Merino, N., Qu, Y., Deeb, R.A., Hawley, E.L., Hoffmann, M.R., Mahendra, S., 2016. Degradation and removal methods for perfluoroalkyl and polyfluoroalkyl substances in water. *Environ. Eng. Sci.* 33(9), 615-649.
- Metcalf, C.D., Koenig, B.G., Bennie, D.T., Servos, M., Ternes, T.A., Hirsch, R., 2003. Occurrence of neutral and acidic drugs in the effluents of Canadian sewage treatment plants. *Environ. Toxicol. Chem.* 22(12), 2872-2880.
- Minten, J., Adolfsson-Erici, M., Björleinius, B., Alsberg, T., 2011. A method for the analysis of sucralose with electrospray LC/MS in recipient waters and in sewage effluent subjected to tertiary treatment technologies. *Int. J. Environ. Anal. Chem.* 91(4), 357-366.
- Mukherjee, A., Zimmerman, A.R., Harris, W., 2011. Surface chemistry variations among a series of laboratory-produced biochars. *Geoderma*. 163(3-4), 247-255.
- Park, S., Zenobio, J.E., Lee, L.S., 2018. Perfluorooctane sulfonate (PFOS) removal with Pd⁰/nFe⁰ nanoparticles: Adsorption or aqueous Fe-complexation, not transformation? *J. Hazard. Mater.* 342, 20-28.
- Parks, G.A., 1965. The isoelectric points of solid oxides, solid hydroxides, and aqueous hydroxo complex systems. *Chem. Rev.* 65(2), 177-198.
- Punyapalakul, P., Suksomboon, K., Prarat, P., Khaodhiar, S., 2013. Effects of surface functional groups and porous structures on adsorption and recovery of perfluorinated compounds by inorganic porous silicas. *Separ. Sci. Technol. (Philadelphia)*. 48(5), 775-788.
- Rahman, M.F., Peldszus, S., Anderson, W.B., 2014. Behaviour and fate of perfluoroalkyl and polyfluoroalkyl substances (PFASs) in drinking water treatment: A review. *Water Res.* 50, 318-340.
- Rajapaksha, A.U., Vithanage, M., Ahmad, M., Seo, D.C., Cho, J.S., Lee, S.E., Lee, S.S., Ok, Y.S., 2015. Enhanced sulfamethazine removal by steam-activated invasive plant-derived biochar. *J. Hazard. Mater.* 290, 43-50.
- Robertson, W.D., Blowes, D.W., Ptacek, C.J., Cherry, J.A., 2000. Long-term performance of in situ reactive barriers for nitrate remediation. *Ground Water*. 38(5), 689-695.

- Rodil, R., Quintana, J.B., Concha-Graña, E., López-Mahía, P., Muniategui-Lorenzo, S., Prada-Rodríguez, D., 2012. Emerging pollutants in sewage, surface and drinking water in Galicia (NW Spain). *Chemosphere*. 86(10), 1040-1049.
- Sanchez, W., Sremski, W., Piccini, B., Palluel, O., Maillot-Maréchal, E., Betoulle, S., Jaffal, A., Aït-Aïssa, S., Brion, F., Thybaud, E., Hinfrey, N., Porcher, J.M., 2011. Adverse effects in wild fish living downstream from pharmaceutical manufacture discharges. *Environ. Int.* 37(8), 1342-1348.
- Schaider, L.A., Rudel, R.A., Ackerman, J.M., Dunagan, S.C., Brody, J.G., 2014. Pharmaceuticals, perfluorosurfactants, and other organic wastewater compounds in public drinking water wells in a shallow sand and gravel aquifer. *Sci. Total Environ.* 468-469, 384-393.
- Scherer, M.M., Richter, S., Valentine, R.L., Alvarez, P.J.J., 2000. Chemistry and microbiology of permeable reactive barriers for in situ groundwater clean up. *Crit. Rev. Environ. Sci. Technol.* 30(3), 363-411.
- Scheurer, M., Brauch, H.J., Lange, F.T., 2009. Analysis and occurrence of seven artificial sweeteners in German waste water and surface water and in soil aquifer treatment (SAT). *Anal. Bioanal. Chem.* 394(6), 1585-1594.
- Scheurer, M., Storck, F.R., Brauch, H.J., Lange, F.T., 2010. Performance of conventional multi-barrier drinking water treatment plants for the removal of four artificial sweeteners. *Water Res.* 44(12), 3573-3584.
- Seo, P.W., Khan, N.A., Hasan, Z., Jhung, S.H., 2016. Adsorptive removal of artificial sweeteners from water using metal-organic frameworks functionalized with urea or melamine. *ACS Appl. Mater. Interfaces.* 8(43), 29799-29807.
- Sharma, V.K., Oturan, M., Kim, H., 2014. Oxidation of artificial sweetener sucralose by advanced oxidation processes: A review. *Environ. Sci. Pollut. R.* 21(14), 8525-8533.
- Sujana, M.G., Soma, G., Vasumathi, N., Anand, S., 2009. Studies on fluoride adsorption capacities of amorphous Fe/Al mixed hydroxides from aqueous solutions. *J. Fluorine Chem.* 130(8), 749-754.
- Tong, A.Y.C., Braund, R., Warren, D.S., Peake, B.M., 2012. TiO₂-assisted photodegradation of pharmaceuticals - A review. *Cent. Eur. J. Chem.* 10(4), 989-1027.
- Toth, J.E., Rickman, K.A., Venter, A.R., Kiddle, J.J., Mezyk, S.P., 2012. Reaction kinetics and efficiencies for the hydroxyl and sulfate radical based oxidation of artificial sweeteners in water. *J. Phys. Chem. A.* 116(40), 9819-9824.
- Van Stempvoort, D.R., Robertson, W.D., Brown, S.J., 2011. Artificial sweeteners in a large septic plume. *Ground Water Monit. R.* 31(4), 95-102.
- Van Stempvoort, D.R., Roy, J.W., Grabuski, J., Brown, S.J., Bickerton, G., Sverko, E., 2013. An artificial sweetener and pharmaceutical compounds as co-tracers of urban wastewater in groundwater. *Sci. Total Environ.* 461-462, 348-359.
- Wang, F., Shih, K., 2011. Adsorption of perfluorooctanesulfonate (PFOS) and perfluorooctanoate (PFOA) on alumina: Influence of solution pH and cations. *Water Res.* 45(9), 2925-2930.
- Williams, M., Martin, S., Kookana, R.S., 2015. Sorption and plant uptake of pharmaceuticals from an artificially contaminated soil amended with biochars. *Plant Soil.* 395(1-2), 75-86.
- Wilson, R.E., 1923. The mechanism of the corrosion of iron and steel in natural waters and the calculation of specific rates of corrosion. *Ind. Eng. Chem.* 15(2), 127-133.
- Yu, J., Lv, L., Lan, P., Zhang, S., Pan, B., Zhang, W., 2012. Effect of effluent organic matter on the adsorption of perfluorinated compounds onto activated carbon. *J. Hazard. Mater.* 225-226, 99-106.

- Zhang, D., Luo, Q., Gao, B., Chiang, S.Y.D., Woodward, D., Huang, Q., 2016. Sorption of perfluorooctanoic acid, perfluorooctane sulfonate and perfluoroheptanoic acid on granular activated carbon. *Chemosphere*. 144, 2336-2342.
- Zhao, H., Cao, Z., Liu, X., Zhan, Y., Zhang, J., Xiao, X., Yang, Y., Zhou, J., Xu, J., 2017. Seasonal variation, flux estimation, and source analysis of dissolved emerging organic contaminants in the Yangtze Estuary, China. *Mar. Pollut. Bull.* 125(1-2), 208-215.
- Zhao, H., Liu, X., Cao, Z., Zhan, Y., Shi, X., Yang, Y., Zhou, J., Xu, J., 2016. Adsorption behavior and mechanism of chloramphenicols, sulfonamides, and non-antibiotic pharmaceuticals on multi-walled carbon nanotubes. *J. Hazard. Mater.* 310, 235-245.
- Zheng, H., Wang, Z., Zhao, J., Herbert, S., Xing, B., 2013. Sorption of antibiotic sulfamethoxazole varies with biochars produced at different temperatures. *Environ. Pollut.* 181, 60-67.

CRedit author statement

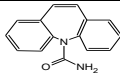
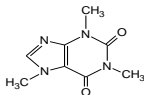
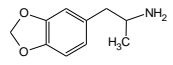
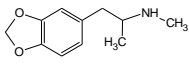
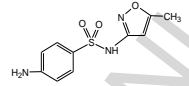
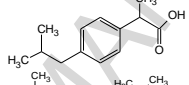
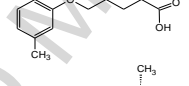
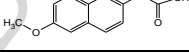
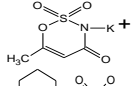
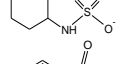
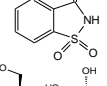
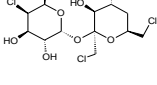
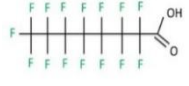
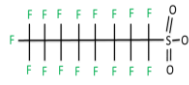
YingYing Liu: Methodology, Investigation, Data curation, Writing – Original Draft, Visualization, Formal Analysis, Project Administration

David Blowes: Conceptualization, Methodology, Resources, Writing – Review & Editing, Project Administration, Funding Acquisition

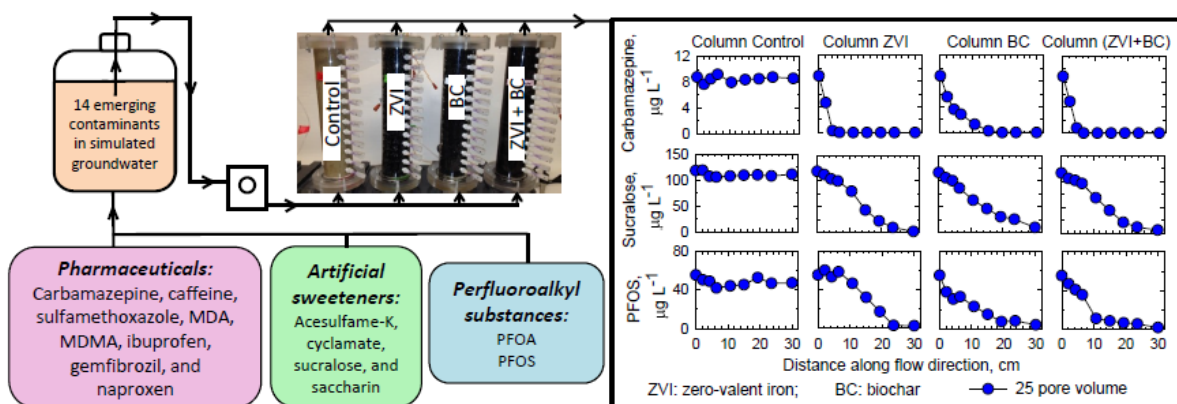
Carol Ptacek: Conceptualization, Methodology, Resources, Writing – Review & Editing, Supervision, Project Administration, Funding Acquisition

ACCEPTED MANUSCRIPT

Table 1 Physicochemical variables for target compounds.

	Target compound	Structure	Character (charge)	pK_a	$\log K_{ow}$	$\log D_{ow}$ at pH=8
Pharmaceutical compound	Carbamazepine (CBZ)		Base (N)	-0.49	2.77	2.77
	Caffeine (CAF)		Base (+)	10.4	-0.07	-2.20
	3,4-methylenedioxyamphetamine (MDA)		Base (+)	9.7	1.43	-0.55
	3,4-methylenedioxymethamphetamine (MDMA)		Base (+)	9.9	1.86	-0.25
	Sulfamethoxazole (SMX)		Acid/Base (-)	1.7, 5.6	0.79	-0.11
	Ibuprofen (IBU)		Acid (-)	4.5	3.84	0.85
	Gemfibrozil (GEM)		Acid (-)	4.8	4.39	1.14
Artificial sweetener	Naproxen (NAP)		Acid (-)	4.2	2.99	-0.36
	Acesulfame-K (ACE-K)		Acid (-)	2.0	-0.69	-3.06
	Cyclamate (CYC)		Acid (-)	1.7	0.61	-1.77
	Saccharine (SAC)		Acid (-)	1.94	0.45	-0.49
Perfluoroalkyl substance	Sucralose (SCL)		Acid (N)	11.9	-0.47	-0.47
	Perfluorooctanoic acid (PFOA)		Acid (-)	0.5	5.11	1.58
	Perfluorooctane sulfonic acid (PFOS)		Acid (-)	-2.3	5.43	3.05

Note: (N): Neutral; (+): Positively charged; (-): Negatively charged. pK_a , $\log K_{ow}$, and $\log D_{ow}$ of target compounds were obtained from Chemicalize.org by ChemAxon (<http://www.chemicalize.org>). The $\log D_{ow}$ (pH dependent $\log K_{ow}$) values reported in this study were for pH 8.



Graphical abstract

Research highlights

- Zero-valent iron and biochar were used in a passive treatment system (four columns)
- Simultaneous removal of 13 emerging contaminants in passive treatment system
- >97% of 8 pharmaceuticals were removed (rate: cationic>neutral>anionic compounds)
- 15-60% of input acesulfame-K and >75% of input sucralose was removed
- Partial removal of PFOA and PFOS; greater removal of PFOS than PFOA